ISSN-1996-918X

Pak. J. Anal. Environ. Chem. Vol. 26, No. 1 (2025) 88 – 104

http://doi.org/10.21743/pjaec/2025.06.13

Comparative Study of Mass Transfer Limitation Steps in Bemacid Yellow and Methyl Red Biosorption: Investigation using Unique and Binary Resistance Models

Fouzia Ouazani*, Mokhtaria Reguig, Khedidja Benouis

Laboratory of Process Engineering, Materials and Environment, Faculty of Technology, University of Djillali Liabes, PO Box 89, Sidi Bel Abbes 22000, Algeria.

*Corresponding author Email: ouazanifouzia@yahoo.fr

Received 21 July 2023, Revised 01 August 2024, Accepted 28 August 2024

Academic Editor: Farah Naz Talpur

Abstract

In this study, brewery waste was employed as an adsorbent to remove two dyes: Bemacid Yellow (BY) and Methyl Red (MR). Optimal operational conditions were determined using the Bach mode. Kinetic data fitting was carried out using pseudo first and second order models. The results revealed that the pseudo second order model exhibited a better fit for both dyes, with a high determination coefficient (R^2=0.99). The single resistance model demonstrated a positive correlation between the initial dye concentration (C_0) and the external mass coefficient (k_f) described by the empirical relationships: $k_{fMR} = 0.00044C_0^{0.65}$ and $k_{f(BY)} = 0.0208C_0^{0.033}$ for MR and BY dyes adsorption, respectively. According to the obtained results from the binary resistances diffusion model, it was determined that pore diffusion played a dominant role in the adsorption process of both dyes. This conclusion was supported by the observed increase in the film diffusion coefficient (D_f) values. On the other hand, alternative formulas indicate that the adsorption processes of BY were primarily controlled by film diffusion. To summarize, the adsorption process of both dyes is influenced by two key steps: pore diffusion and film diffusion. This analysis provides insights into the significance of each parameter and their respective contributions to the overall adsorption mechanism.

Keywords: Bemacid Yellow, Methyl Red, Kinetic models, Mass transfer, Binary resistance

Introduction

The dye industry is associated with the discharge of organic pollutants known to be toxic, posing harmful effects on human health and aquatic life. These pollutants have been proven to cause acute disturbances in aquatic organisms. When these organisms are transferred to the human body by food or by other means, the pollutants absorbed by the latter can lead to a range of physiological disorders, including cramps, hypertension and kidney damage [1]. Consequently, it is imperative to take steps to treat these effluents before their discharge into the environment. [2].

A diverse range of treatment methods, including biodegradation, membrane separation, biosorption, chemical precipitation, coagulation, extraction, and advanced oxidation processes, have been employed for the treatment of colored wastewater [3-4]. The process of adsorption offers a simple and effective treatment method for removing pollutants from contaminated solutions. By

facilitating contact between the polluted solution and an adsorbent surface, the adsorption process proves to be particularly efficient. Moreover, utilizing environmentally friendly and economically viable adsorbents further enhances its effectiveness. In order to meet the requirements of the adsorption process, researchers are actively exploring and investigating diverse adsorbents that are both environmentally friendly and cost-effective. Several studies have focused on highlighting the efficiency of adsorption in removing methyl red (MR) [5-6] from aqueous solutions. Similarly, additional studies have targeted the use of low-cost adsorbents for the efficient treatment of bemacid yellow (BY) [7] through adsorption. This endeavor aims to expand the range of available options and ensure the satisfaction of this process [8-9]. There are several cost-effective natural adsorbents available, including Cotton [10], Jackfruit peel [11], Date stone [12], and Sawdust [13]. Previous studies in the literature have employed batch experiments to examine the kinetics, isotherms, and thermodynamics of sorption processes [14]. However, there is a dearth of comprehensive research focusing on the intricate adsorption mechanism involving both external and internal mass transfer.

Mass transfer forms the basis of various separation processes in the realm of chemical engineering, wherein the material balance of each compound is given due consideration [15]. This study aims to provide a detailed analysis of the adsorption process by determining the rate of separation that occurs during its operation. Given that dyes adsorption is a time-dependent process, it becomes essential to ascertain the adsorption rate for effective control of the process, as well as for the design and evaluation of suitable adsorbents utilized in this operation. The migration of dyes from the liquid phase to the solid phase is facilitated by a mass transfer gradient spanning across both phases [16]. This study focuses on examining the adsorption process specifically from the aqueous phase, which involves the following sequential steps: (i) Solute transport from bulk solution to the film surrounding the adsorbent (film diffusion).

(ii) Solute transport from the film to the adsorbent pores (internal diffusion) (iii) Adsorption of the solute on the external surface of the adsorbent through binding of the ions to the active sites [1, 3]. Among these steps, the one that exhibits a longer duration will govern the overall process and serve as the rate-limiting step.

Previous research has indicated that in the presence of porous adsorbents, the dominant mechanism controlling the adsorption process is intraparticle diffusion. [16]. In their research, Yuan et al. [17] focused on investigating the adsorption of CO_2 using a batch mode. They aimed to estimate the diffusion coefficient, which required the utilization of numerical resolution techniques due to the complex nature of the nonlinear equations involved. Mamdouh et al. [18] established correlations between the external diffusion coefficient, pollutant concentration, and adsorbent weight, as well as the relationship between the internal diffusion coefficient and these same parameters. These results were derived when applying a single resistance mass-transfer model.

The current study employed brewery waste as an adsorbent to remove MR and BY dyes from an aqueous medium. The composition of the adsorbent was analyzed using an X-ray fluorescence (ED-XRF) spectrometer. Various operational parameters, including pH of the medium, contact time, adsorbent weight, and initial dye concentration, were investigated to determine their effects on the adsorption capacity. Also, the goal of this study was to utilize both single and binary resistances mass transfer models to

accurately predict diffusion coefficient values and identify the limiting step in the process of dyes biosorption. Additionally, the study aimed to examine the effects of the operational parameters on the diffusion coefficient and determine whether they had a positive or negative impact.

Materials and Methods

Raw Material and Adsorbat

Brewery waste: is an industrial waste was obtained from local breweries (Ain temouchent-west of Algeria). Distilled water (pH range from 6.5 to 6.8) was used to wash samples in order to decline existent impurities; this operation was repeated several times. After this step, the biomaterial was dried in oven at 80 °C during 48 h. The dried biomass was ground to a fine powder; sieved to obtain average sizes (250 µm).

BY is an industrial dye classified under the ETL dye family. It is widely utilized in the Algerian textile industry due to its remarkable fixing capacity. However, the exact chemical structure of this dye remains unknown. For this study, a stock solution was prepared by diluting 1 g of the BY dye in 1 liter of distilled water.

The MR used in this study is an Azo dye has 269.29 g/ mol molecular weight and C.I 13020 was purchased from Biochem Chemopharma – France. The stock solution for the tested concentrations was prepared using the same procedure as the BY solution, followed by subsequent dilutions to achieve the desired concentrations. The choice of these two dyes was made due to their widespread utilization in industrial applications.

Chemicals and Reagents

All chemicals and reagents utilized in this study were of analytical grade. Sodium hydroxide (NaOH, 98%) and hydrochloric acid (HCl, 37%) were obtained from Sigma-Aldrich. Distilled water was used exclusively in all experimental procedures.

For elemental analysis of the biosorbent, an Energy Dispersive X-ray Fluorescence (ED-XRF) spectrometer from Bruker was employed. The spectrometer was equipped with a Rhodium X-ray tube and an X-Flash® SDD detector.

Sample Preparation

The adsorption studies were conducted in batch mode, where samples were subjected to a mono-parametric study involving varied operational conditions. These conditions included contact time ranging from 5 to 60 min, adsorbent masses of 50 mg and 100 mg, initial dye concentrations ranging from 5 mg/L to 100 mg/L for MR (with weak solubility in distilled water up to 100 mg/L) and from 5 mg/L to 500 mg/L for BY, and pH of the solution ranging from 2 to 11. A fixed volume of 50 mL of each dye solution was mixed with the specified amount of adsorbent in stoppered flasks. The mixture was agitated at room temperature (298 ± 2 K) at fixed speed 240 rpm. Following the adsorption process, the solution was subjected to filtration. The concentration of the remaining dyes was subsequently analyzed using a UV-visible spectrophotometer (HACH-DR 2000). For MR dye, the absorbance was measured at 520 nm in acidic medium and 430 nm in basic medium. As for BY dye; the absorbance was measured at 420 nm. pH measurements of the solution were conducted using a pH meter (SCHOTT CG711).

Adsorption Optimization Using Different Models

Adsorption Optimization

The adsorption capacity (q_e, $mg.g^{-1}$) and R% percent removal of dyes were calculated using eqs. (1) and (2) [9]:

$$q_e = \frac{C_0 - C_e}{m} V \quad (1)$$

$$R\ \%\ removal = \frac{C_0 - C_e}{C_0} 100 \quad (2)$$

Where C_0 and C_e are the initial and equilibrium concentrations ($mg.L^{-1}$), respectively of the dyes solution, V is the volume (L), and m is the mass (g) of the adsorbent.

Kinetic Optimization

The commonly employed kinetic models for interpreting the adsorption mechanism include the pseudo-first order and pseudo-second order models. The pseudo-first order model is characterized by the rearranged linear form eq. [9]:

$$Ln(q_e - q_t) = Lnq_e - k_1 t \quad (3)$$

And the linear equation form of pseudo-second order model can be expressed by [9]:

$$\frac{t}{q_t} = \frac{1}{kq_e^2} + \frac{1}{q_e} t \quad (4)$$

Where: q_e and q_t represent the adsorption capacity at equilibrium and time 't' respectively. k_1 and k_2 were the pseudo-first (min^{-1}) and second order (g/mg.min) rate constants, respectively.

Single Resistance Diffusion Model

The application of this model involves two assumptions. The first assumption assigns more significance to external mass transfer and overlooks intra-particle diffusion. Conversely, the second assumption prioritizes intra-particle transfer and disregards external mass transfer.

a-External Mass Transfer Model

When the samples were subjected to medium agitation speed, mass transfer resistance takes place in the film surrounding the adsorbent particles. However, when the stirring speed is excessively high, the boundary layer around the particles is disrupted. To maintain the integrity of the boundary layer film, a stirring speed of 240 rpm was employed in this study. The eq. (5) establishes the conventional relationship between the concentration variation and the external mass transfer coefficient [19].

$$k_f S_s = -\left[\frac{dC_t/C_0}{dt}\right]_{t\to 0} \quad (5)$$

Where S_s is the specific surface of the brewery waste determined by the following equation:

$$S_s = \frac{6m_s}{d\rho_s(1-\varepsilon)} \quad (6)$$

Where: ε particle voidage, ρ_s solid density (g/cm^3), d particle diameter (m) and m_s concentration of adsorbent g/cm^3. McKay et al. [20] provides an alternative general form to determine k_f under any conditions:

$$k_f = A(variable)^B \quad (7)$$

By taking the logarithmic form of eq. (7), a linear relationship can be obtained, allowing for the determination of the slope (B) and intercept (A) from the resulting straight line. Hence, the coefficient can be determined by drawing a tangent through the origin on the curve of Ct / Co versus t.

b-Intra-particle Diffusion Model

Weber and Morris equation was utilized to test the single rate-controlling step in this study [18]:

$$q_t = k_{in} t^{0.5} \quad (8)$$

Binary Resistances Diffusion Effects on Adsorption Process

The effective diffusivity in non-homogeneous media, accounting for both surface film diffusion and pore diffusion, can be represented by the equation below [15]:

$$D_{eff} = \mathrm{D_p} + \rho_s \mathrm{D}_f \frac{\partial \mathrm{q_e}}{\partial \mathrm{C_e}} \quad (9)$$

The derivative term $\frac{\partial \mathrm{q_e}}{\partial \mathrm{C_e}}$ in equation (9) corresponds to the slope of the isotherm curve. $\mathrm{D_p}$ and $\mathrm{D_f}$ denote the coefficients of pore diffusion and film diffusion, respectively.

Results and Discussion

Characterization of Adsorbent

The chemical composition of the biosorbent as determined by XRF indicates that the calcium (Ca) with 1.44% ± 0.03 was the major inorganic constituents of our biomass, and in second position the iron (Fe) at 0.054% ± 0.006, while chloride (Cl), titanium (Ti), manganese (Mn), nickel (Ni), copper (Cu), zinc (Zn), bromine (Br) and lead (Pb) were abundant constituents at 0.015% ± 0.008, 0.0018% ± 0.0007, 0.012% ± 0.005, 0.0028% ± 0.0008, 0.0035% ± 0.0013, 0.0057% ± 0.0007, 0.0009% ± 0.0003 and 0.00015% ± 0.0009, respectively, and which may be play an important role in sorption process via ion-exchange mechanism.

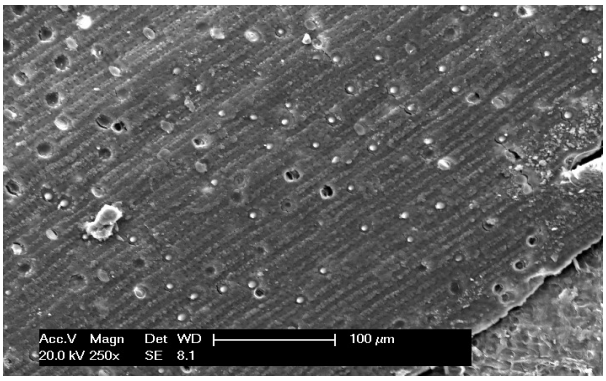

Figure 1. **SEM images of brewery waste**

From our previous research [8], the results of FTIR classify the brewery waste as lignocellulosic sorbent. Fig. 1 presents the SEM image of the adsorbent. SEM image revealed that the surface of the adsorbent contains numerous porous (Fig.1).

Optimization of Biosorption Operational Conditions

The pH of the solution is considered one of the crucial operating conditions that greatly influence the biosorption process. In particular, the pH level has a significant impact on both the biosorbent and the adsorbate behavior in the aqueous solution. For instance, the MR dye, being an azo dye, exhibits a red color with a maximum wavelength (λ_{max}) of 520 nm in acidic conditions, while it displays a yellow color with a λ_{max} of 430 nm in basic conditions. When the pH of the solution is raised from 2 to 4 as depicted in Table 1, the adsorption capacity of MR dye exhibits a noticeable enhancement. At a contact time of 1 h, the adsorption capacity values for MR dye escalate from 25 mg/g to 42.5 mg/g. Following this, there was a decrease in the adsorption capacity of MR dye, ranging from 28.2 mg/g to 13.4 mg/g as depicted in Table 1, as the pH of the solution was increased from 7 to 8 while maintaining the same stirring time. However, the adsorption capacity shows an increase once again when the pH of the medium was raised to 11.

Notably, the highest observed adsorption capacity (qe = 42.5 mg/g) is attained in an acidic medium with a pH of 4, as evidenced by the obtained results from this study. To elucidate this observed increase, two key parameters need to be considered: the pH at the point of zero charge ($\mathrm{pH_{pzc}}$) of the biosorbent and the acid dissociation constant ($\mathrm{pK_a}$) of the adsorbate.

Table.1. **Effects of pH solution and contact time on MR dye adsorption capacity (λ_{max} =520 nm, C_{0MR} =50 mg/L and T=298 ± 1 °C).**

Time (min)	qe					
	pH=2	pH =3	pH =4	pH =7	pH =8	pH =11
0	0	0	0	0	0	0
5	24.2	26.2	34.2	7.6	4	29
10	31.2	35.2	41.3	4.2	5.5	35.4
15	33.1	36.1	42.8	21.6	7	37.7
20	34.4	37.2	42.8	29.3	10.5	38.1
30	35.2	38.1	42.9	28.2	12.5	37.7
40	34.6	37.8	43.1	28.4	14.5	37.1
50	36.1	39.2	42.9	28.12	14	37
60	35.6	38.2	42.9	28.2	13.5	36.9

In our previous study [8], the pH_{pzc} of the brewery waste was determined to be 6.1. This indicates that when the pH of the solution is below the pH_{pzc}, the surface of the biosorbent carries a positive charge. Conversely, when the pH exceeds the pH_{pzc}, the biosorbent surface becomes negatively charged. The pK_a value of MR dye is reported as 5.1 [21]. Similar to the behavior of the biosorbent surface, the MR molecule exhibits changes in charge depending on the pH of the medium relative to its pK_a value. When the pH is below the pK_a, the MR molecule carries a positive charge, whereas it becomes negatively charged as the pH exceeds the pK_a. The observed increase in dye removal can be attributed to the favorable interaction between the positive surface charge of the biosorbent and the negatively charged MR molecules when the pH is lower than both the biosorbent's pH_{pzc} and the dye's pK_a. In this study, a pH value of 4 was found to be optimal for MR dye removal.

Based on the data presented in Fig. 2, the adsorption capacity of BY dye exhibits a noticeable increase from 17.2 mg/g to 46.2 mg/g as the contact time extends from 5 min to 60 min at pH 2. Conversely, with an increase in pH solution from 2 to 11 while maintaining a constant stirring time of one hour, the adsorption capacity decreases from 46.2 mg/g to 3.91 mg/g. These results clearly indicate that the acidic medium is more favorable for the efficient removal of BY dye. Therefore, based on these results, it can be concluded that the optimum pH solution for the removal of BY dye is determined to be 2, considering its significantly higher adsorption capacity in this acidic condition.

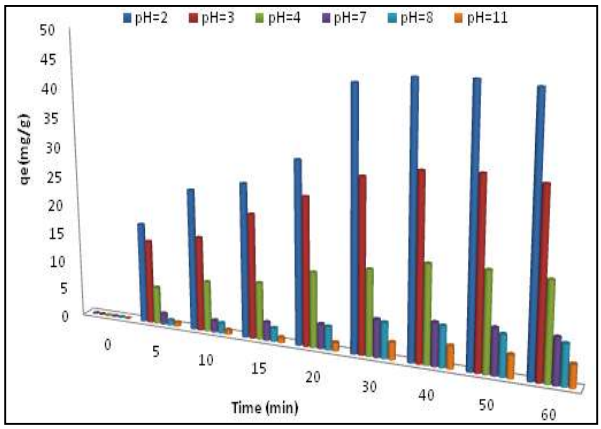

Figure 2. **pH solution and contact time effects on BY dye adsorption capacity (λ_{max} =420 nm, C_{0BY}=50 mg/L and T=298 ± 1 °C)**

The impact of two additional important parameters, contact time and adsorbent mass, was also examined. The results, depicted in Fig. 3 and Fig. 4, demonstrate distinct patterns

in the adsorption process. Notably, within the initial five minutes, a rapid adsorption phase was observed, which is succeeded by a moderate rate of adsorption up to fifteen minutes.

Finally, the system reaches a slower phase corresponding to the equilibrium state. The collective results suggest that the adsorption of MR and BY dyes can be characterized as a rapid process. This observation holds true for both the effect of time and the different steps involved in the adsorption capacity, as depicted in Fig. 2, 3, and 4. On the other hand, when removing MR using activated carbon derived from moringa, the process proved to be exceedingly slow, extending beyond treatment duration of 2 h [22]. Furthermore, the influence of adsorbent mass on the adsorption capacity is demonstrated in Fig. 3 and 4. It is evident that an increase in adsorbent mass leads to a decrease in the adsorbent's affinity for both BR and BY dyes. Specifically, the adsorption capacity decreases from 46 mg/g to 21 mg/g for BR dye and from 48.2 mg/g to 38.3 mg/g for BY dye when the adsorbent mass was increased from 50 mg to 100 mg. This decrease can be attributed to the accumulation and aggregation of the adsorbent particles. Therefore, the optimal adsorbent mass for the subsequent experiments was determined to be 50 mg. These results are consistent with previous studies that utilized brewery waste for the removal of BR dye [8].

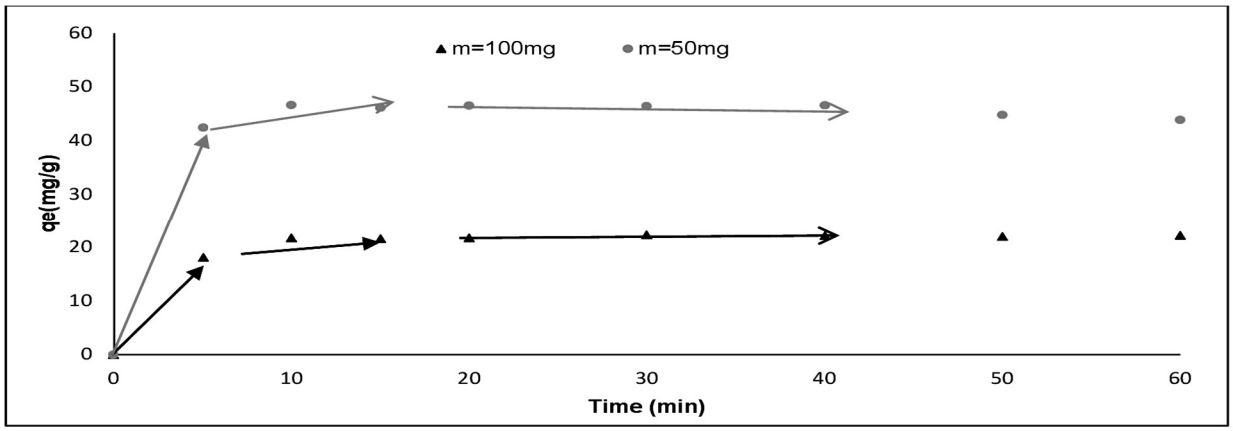

Figure 3. **Adsorbent weight and time effects on MR dye adsorption capacity (C_{0MR}=50 mg/L, pH=4 and T=298 ± 1 °C)**

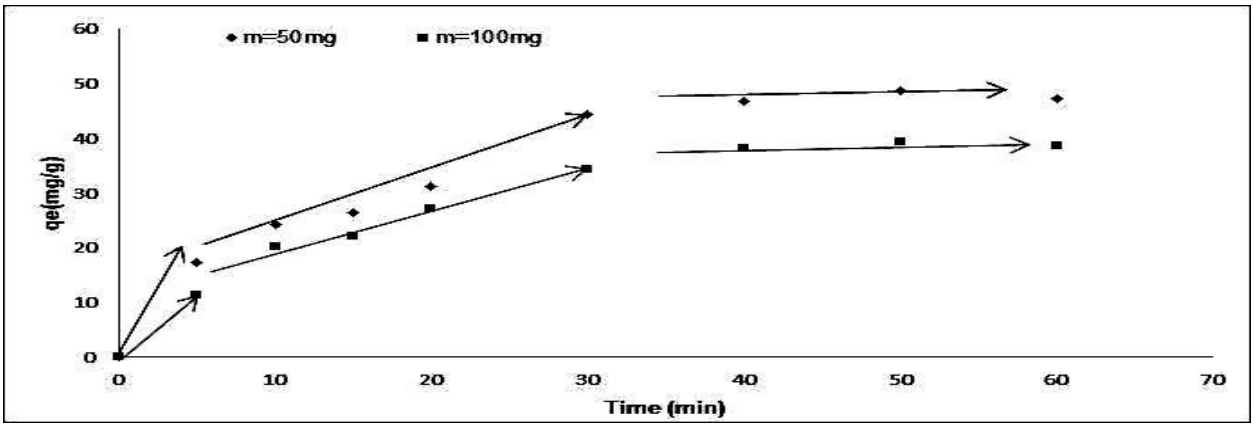

Figure 4. **Adsorbent weight and time effects on BY dye adsorption capacity (C_{0BY}=50 mg/L, pH=2 and T=298 ± 1°C)**

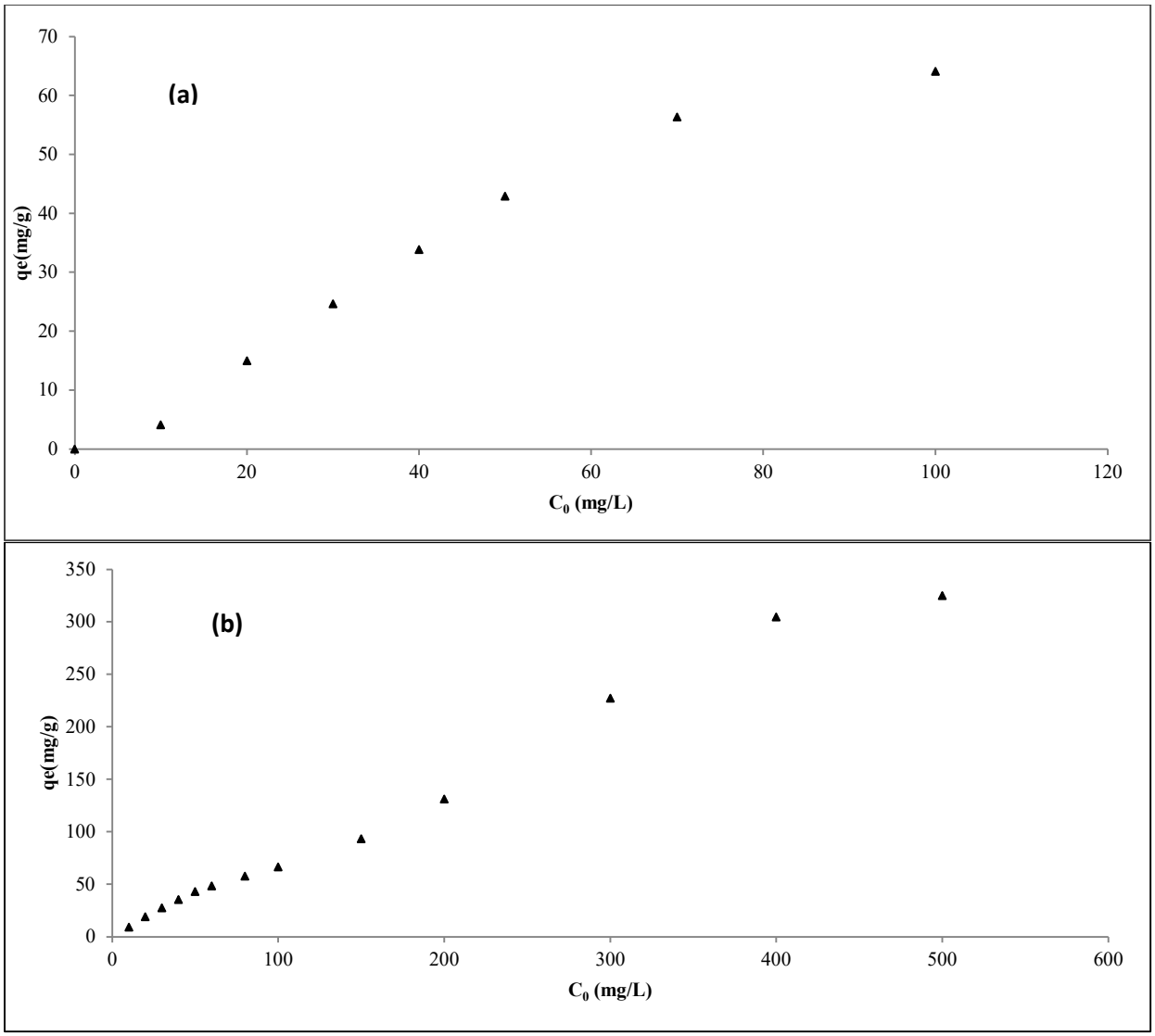

Figure 5. **Plot of initial dye concentration (a) effect on MR dye adsorption capacity (pH=4, m=50 mg and T=298± 1°C); (b) effect on BY dye adsorption capacity (pH=2, m=50 mg and T=298± 1°C)**

The impact of the initial dye concentration on the adsorption capacity was also examined in this study. From Fig. 5a, it can be observed that the adsorption capacity shows a significant increase for low dye concentrations, as indicated by the steep slope of the curve. However, as the dye concentration reaches 50 mg/L, the slope of the curve decreases, indicating a decrease in the adsorption capacity. The maximum adsorption capacity of MR dye by the adsorbent was found to be 72 mg/g. This decrease in adsorption capacity can be attributed to the limited number of active sites on the adsorbent surface relative to the number of dye molecules in the solution. Due to the low solubility of the dye in distilled water, the experimental tests were stopped at a concentration of 100 mg/L. Similarly, Fig. 5b shows the effect of initial dye concentration on the adsorption capacity in the case of BR dye. The adsorption capacity increases from 18.9 mg/g to 325 mg/g as the initial dye concentration increases from 10 mg/L to 500 mg/L. Furthermore, the adsorption capacity of BY dye follows a comparable pattern, with a maximum adsorption capacity recorded at 327 mg/g.

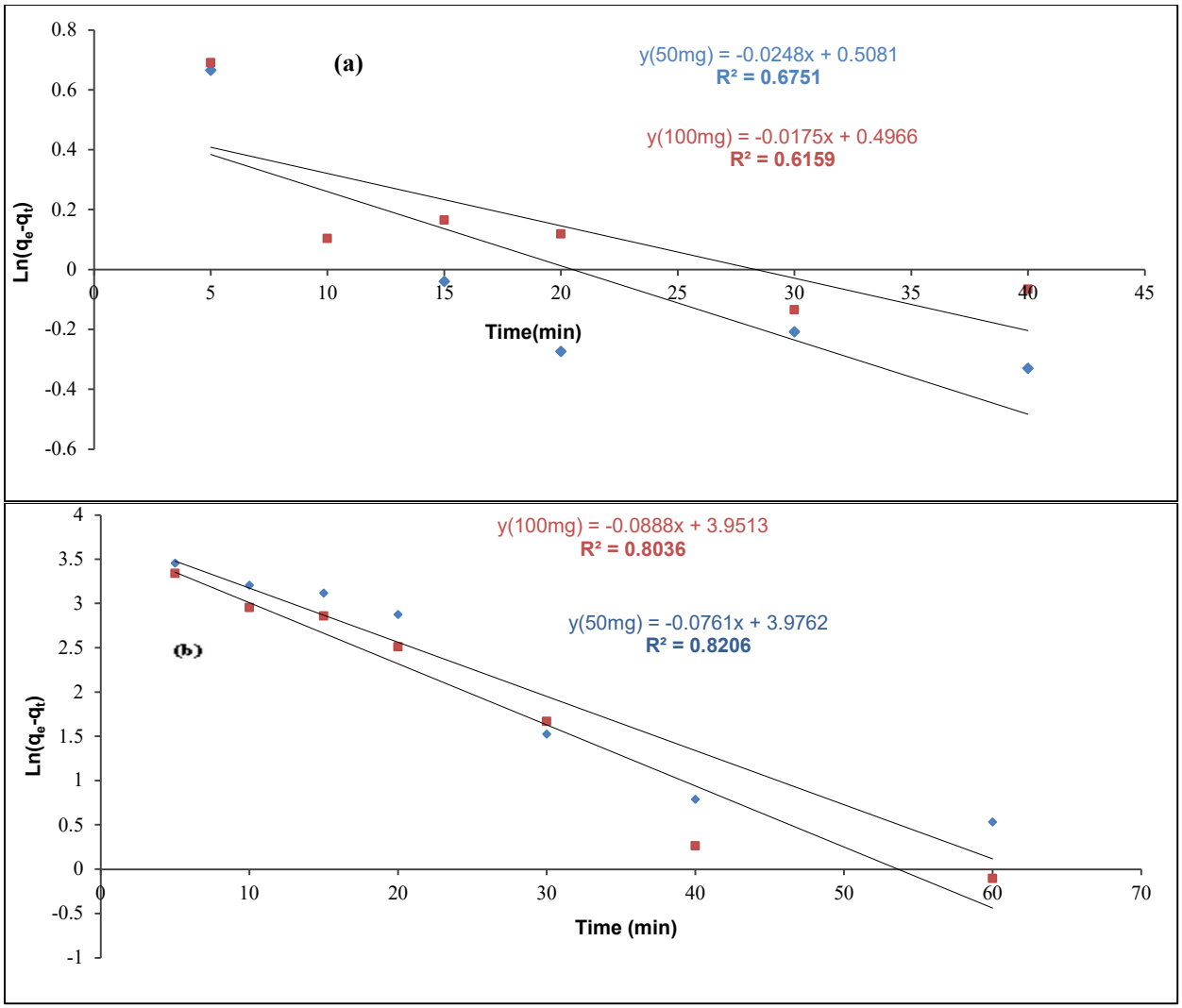

Figure 6. **Plot of pseudo first order model: (a) for MR dye and (b) for BY dye**

Kinetic Study

By applying the two linear forms of eq. (3) and eq. (4), two graphs were generated, as depicted in Fig. 6 and Fig. 7. The initial observations indicate a good fit of the experimental results with the pseudo-second order model. This is further supported by the determination coefficient values presented in Table 2, where the determination coefficient R^2 value for the pseudo-second order model was higher compared to the pseudo-first order model. Moreover, the estimated adsorption capacity values obtained from the model align closely with the experimental adsorption capacity values, reinforcing the validity of these initial observations.

The adsorption capacities estimated by the pseudo second-order model were 44.24 mg/g and 22.42 mg/g, while the corresponding experimental values were 46 mg/g and 21 mg/g. These results were obtained when the mass of the adsorbent was increased from 50 mg to 100 mg. The results of Maiyalagan et al. [1] and Srivastava et al. [23] suggest that when the adsorption kinetics follows the pseudo second-order model, it implies a chemisorption-based rate-limiting sorption step. However, Hubbe et al. [24] observed that

for cellulosic adsorbents, if the experimental data fits well with the pseudo-first-order model, it indicates that the adsorption mechanism is primarily limited by external mass diffusion. However, the pseudo-second-order model does not provide specific information about which mechanism represents the rate-limiting step. To ascertain the controlling diffusion mechanism in MR and BY dyes adsorption, the influence of both external and internal mass transfer resistances on the process was examined separately as well as in combination.

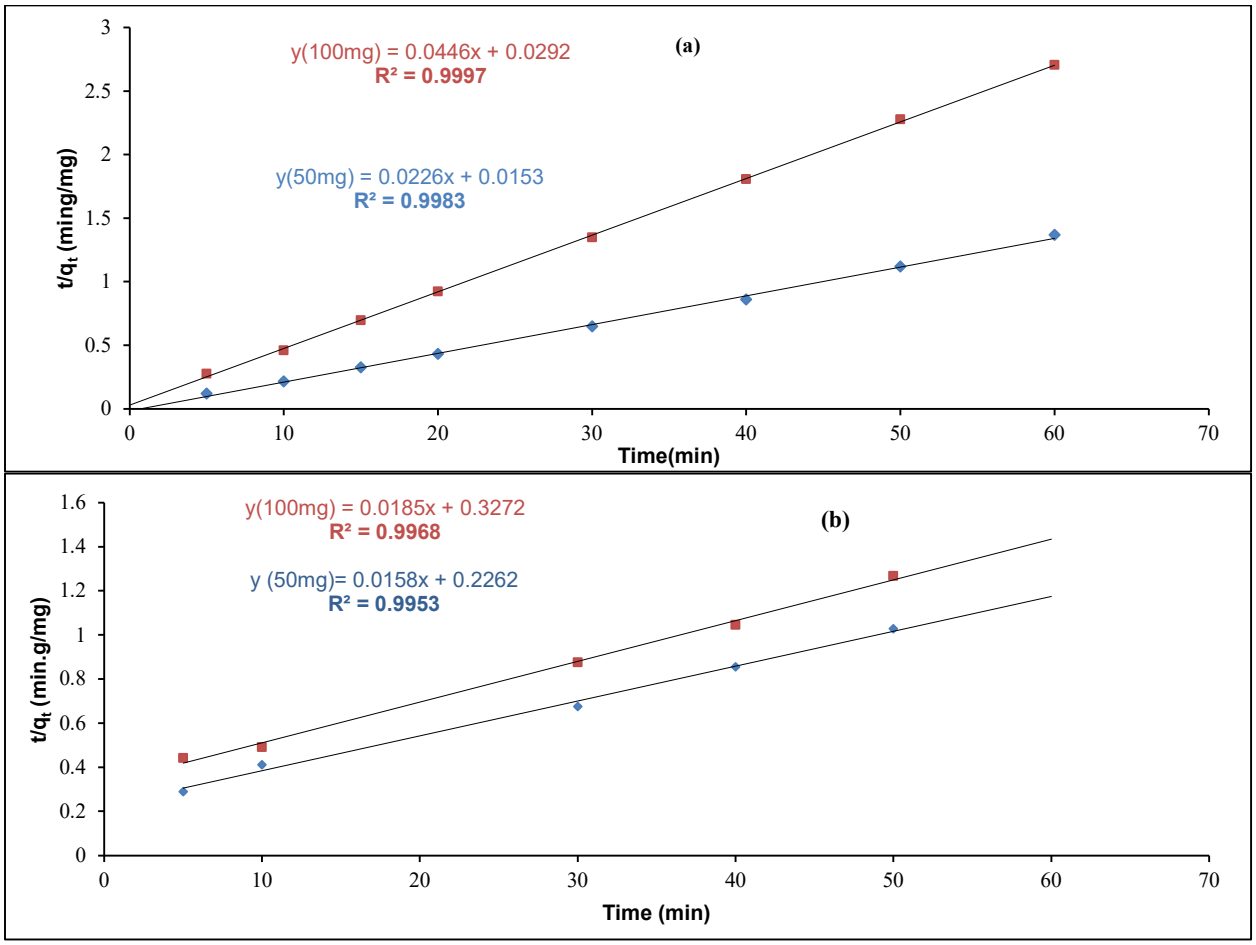

Figure 7. **Plot of pseudo second order model: (a) for MR dye and (b) for BY dye**

Table 2. **Kinetic parameter of dyes removal**

Dye concentration (mg/L)			50	
qe (experimental) (mg/g)	46	21	48.6	39.5
Mass adsorbent (mg)	50	100	50	100
Dye	MR		BY	
Pseudo first order model				
k_1 (min^{-1})	0.024	0.017	0.076	0.088
qe (mg/g)	1.66	1.64	52.00	52.01
R^2	0.675	0.615	0.86	0.80
Pseudo second order model				
k_2 (g/mg.min)	0.033	0.068	0.0011	0.0010
qe (mg/g)	44.24	22.42	63.29	54.04
R^2	0.998	0.999	0.995	0.996

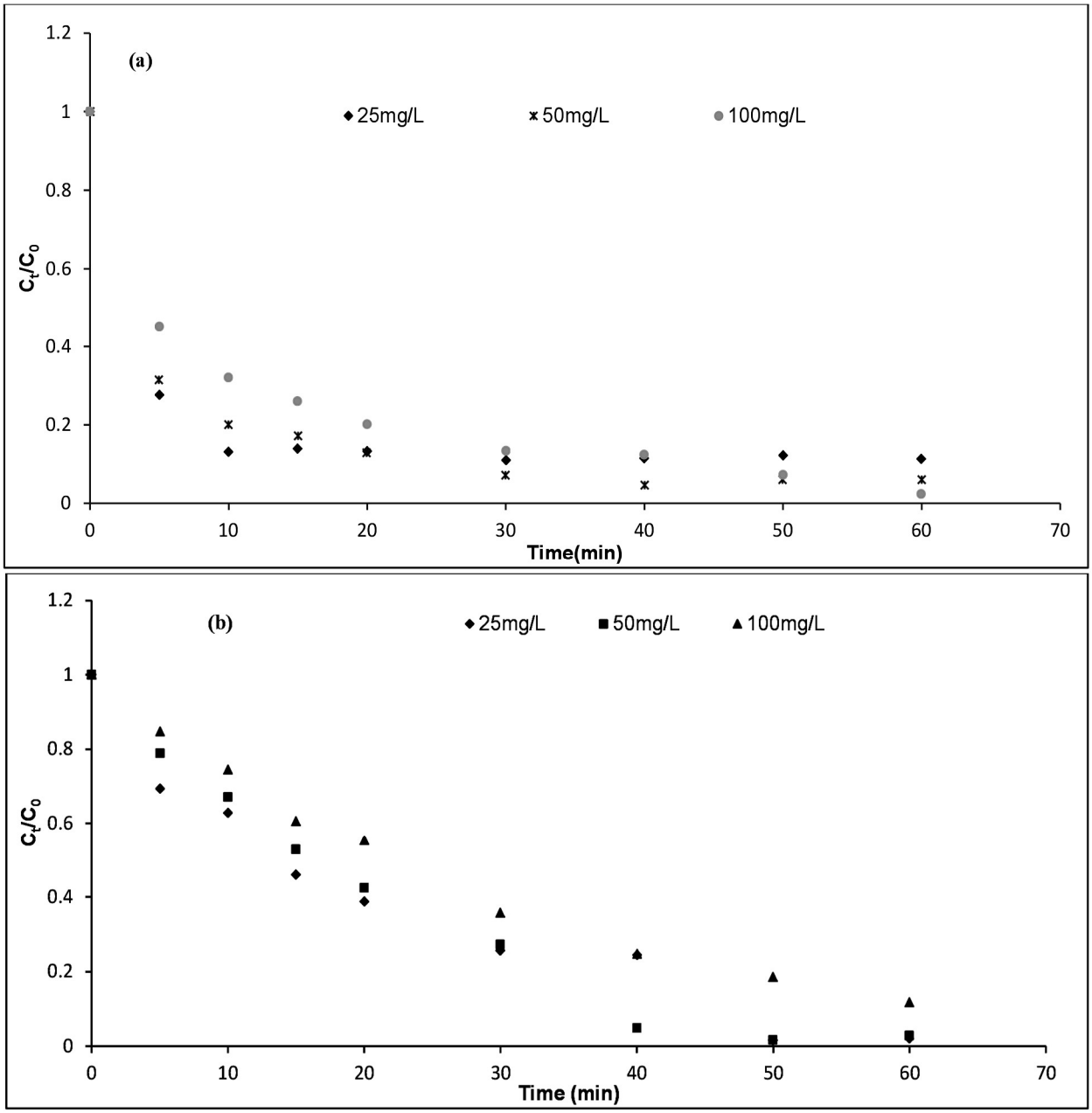

Figure 8. **Effect of initial dye concentration on external mass transfer coefficient: (a) for MR dye and (b) for BY dye**

Results of Single Resistance Diffusion Effect

The results shown in Fig. 8 demonstrate that the slopes of the linear portions of the curves for lower dye concentrations (25 mg/L and 50 mg/L) are nearly identical to the slope obtained for the higher concentration (100 mg/L). The linear representation of eq. (7) successfully correlates with the experimental data, indicating a good fit between the model and the observed results.

$$k_{f(MR)} = 0.00044C_0^{0.65} \quad (10)$$

$$k_{f(RY)} = 0.0208C_0^{0.033} \quad (11)$$

The obtained coefficient value A (0.00044) in the derived relationship of eq. (10) for MR dye falls within a similar range as the value (0.0006) reported by Mamdouh et al. [18] for the adsorption of phenolic compounds using rice husk. However, the coefficient value B (0.65) in our study differs significantly from the reported value in the same study, indicating the notable influence of MR dye concentration on the external mass transfer coefficient. Additionally, in eq. (11), the A value (0.02) obtained aligns with the range (0.08) of results obtained by El-Geundi et al. [25] for the adsorption of basic red 22 dye using maize cob, highlighting the consistency of our results with previous research.

The plot in Fig. 9 illustrates the relationship described by eq. (8). If the straight line passes through the origin, it indicates that intra-particle diffusion is the controlling factor in the adsorption process. When the straight line consists of two linear sections, it suggests that the adsorbent has a diverse range of pore sizes, encompassing meso, macropores, and possibly micropores.

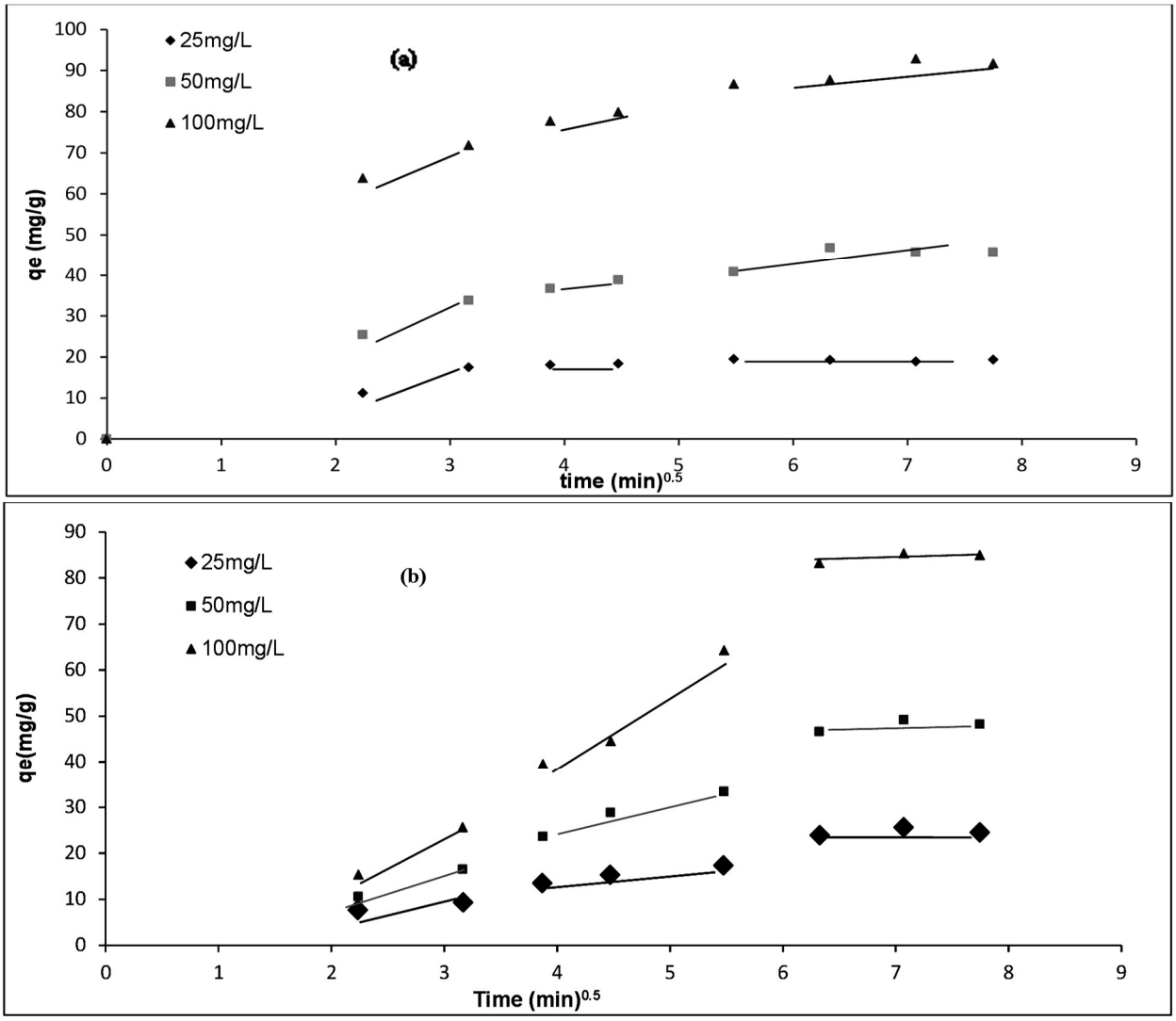

Figure 9. **Weber and Morris intra-particle model: (a) for BR dye and (b) for BY dye**

The observation from Fig. 9 indicates that none of the three curves are straight lines passing through the origin. This suggests that both modes of diffusion play a role in the biosorption process of the dyes.

The observations depicted in Fig. 9 reveal a consistent pattern among all the curves, characterized by three distinct regions. These regions consist of two linear segments that rise gradually, followed by a curved plateau. This pattern can be interpreted as follows: the linear segments correspond to intra-particle diffusion, while the plateau represents the equilibrium state, indicating the complete saturation of the brewery waste surface with dye molecules [26]. The slope of each linear portion provides information about the rate adsorption [27].

According to the results of Cheung et al. [27], the observed three segments can be interpreted as follows:

- The initial segment, characterized by a rapid increase, corresponds to the diffusion of dyes from the bulk solution to the external surface of the adsorbent. This step occurs swiftly.

- The presence of mesopores on the adsorbent surface leads to the second segment, which exhibits a slower slope compared to the first step. It signifies the diffusion of dyes within these mesopores.

- The final segment, with the lowest slope, represents the adsorption occurring in the micropores. This indicates that the diffusion within the micropores is the limiting factor in the overall adsorption process for both dyes.

By examining the slopes of these segments, it can be concluded that the diffusion within the micropores is the rate-determining step for the adsorption of both dyes.

The analysis of the intra-particle diffusion coefficient, conducted in a manner consistent with the assessment of the external mass coefficient, yielded a relationship that depicts its dependence on dye concentration. The obtained results can be summarized by the following equation:

$$k_{int\ (MR)} = 0.322C_0^{0.81} \quad (12)$$

$$k_{int\ (BY)} = 0.142C_0^{1.0036} \quad (13)$$

The analysis of the obtained eq. (8) and (9) for external diffusion, as well as eq. (12) and (13) for intra-particle diffusion, reveals a notable influence of the initial dye concentration on the diffusion coefficient. This effect is particularly pronounced in the case of intra-particle diffusion for both BR dye and BY dye. These findings are consistent with the results reported by Cheung et al. [27] during the adsorption of AR73 using chitosan, where similar trends were observed with A = 0.89 and B = 1.09.

Result of Binary Resistances Diffusion Effect

The diverse formulas cited below allow to calculate the coefficient of the diffusion coefficients, D_p and D_f:

$$n\ \frac{1}{1-F\ (t)^2} = \frac{\pi}{r} D_p.t\ [2] \quad (14)$$

$$\text{With: } F(t) = \frac{q_t}{q_e}\ t_{1/2} = 0.03\frac{r^2}{D_p}\ [28] \quad (15)$$

$$\text{And } t_{1/2} = \frac{1}{k_2 q_e} 1 - \frac{q_t}{q_m} = \frac{6}{\pi^2} \exp\left(-\frac{D_p \pi^2}{r^2}\right) t\ [15] \quad (16)$$

$$t_{1/2} = 0.28\frac{r\delta C_s}{D_f C_e}\ [29] \quad (17)$$

$$log(q_m - q_t) = \log(q_m) - \frac{D_f}{2.303} t \text{ [15]} \quad (18)$$

$$\frac{q_t}{q_e} = 6\left(\frac{D_f}{\pi A^2}\right)^{1/2} t^{1/2} \text{ [2]} \quad (19)$$

Where δ is the film thickness (10^{-3} cm), $\frac{C_s}{C_e}$ is the equilibrium loading of the adsorbent and k_2 is pseudo second order constant. By considering the range of values reported by various authors, we can identify the controlling step that governs the adsorption process.

According to previous studies [15, 19], it has been suggested that film diffusion (D_f) may be the controlling step if the film diffusion coefficient falls within the range of 10^{-6} to 10^{-8} cm^2/s. On the other hand, when the pore diffusion (D_p) is identified as the rate-limiting step, the pore diffusion coefficient should be in the range of 10^{-11} to 10^{-13} cm^2/s [20]. It is important to note that other research [17] indicates that pore diffusion governs the adsorption process when the D_p values are around 10^{-10} cm^2/s. In this study, the adsorbent has a spherical geometry with an average particle size of 250 µm ($r = 0.0125 \times 10^{-4}$ cm). The application of the equations (14 to 19), gives the results grouped in the Table 3.

Based on the values presented in Table 4, it can be observed that the D_p values obtained from Equation (11) fall within the range of 10^{-11} cm^2/s to 10^{-13} cm^2/s. This indicates that pore diffusion is the rate-limiting step in the adsorption process of MR, as compared to the values obtained from eq. (14) and (16). Additionally, the D_p values decrease from 4.7×10^{-8} to 2.9×10^{-8}, from 10^{-12} to 6.4×10^{-13}, and from 1.4×10^{-9} to 9.1×10^{-10} as the dye concentration increases from 25 mg/L to 100 mg/L for eq. (14), (15), and (16), respectively.

Table 3. **Values of pore and film diffusion coefficients for MR dye.**

Equation	**Eq (14)**			**Eq (15)**			**Eq (16)**		
Dye concentration	**25 mg/L**	**50 mg/L**	**100 mg/L**	**25 mg/L**	**50 mg/L**	**100 mg/L**	**25 mg/L**	**50 mg/L**	**100 mg/L**
Coefficients of Equation	**Slope**			**$t_{1/2}$**			**Slope**		
	0.111	0.061	0.076	1.5	3.59	2.43	-0.92	-0.65	-0.57
D_p	$4.7.10^{-8}$	$2.5.10^{-8}$	$2.9.10^{-8}$	$1.\ 10^{-12}$	$4.3.10^{-13}$	$6.4.10^{-13}$	$1.4.10^{-9}$	$1.\ 10^{-9}$	$9.1.10^{-10}$
Equation	**Eq (17)**			**Eq (18)**			**Eq (19)**		
Coefficients of Equation	**$t_{1/2}$**			**Slope**			**Slope**		
	1.5	3.59	2.43	-0.06	-0.02	-0.02	0.23	0.21	0.22
D_f	$8.8.10^{-7}$	$1.5.10^{-6}$	$1.8.10^{-6}$	$1.4.10^{-1}$	$4.7.10^{-2}$	$4.7.10^{-2}$	$2.02.10^{-9}$	$2.3.10^{-9}$	$2.1.10^{-9}$

Table 4. **Values of pore and film diffusion coefficients for BY dye.**

Equation	**Eq (14)**			**Eq (15)**			**Eq (16)**		
Dye concentration	**25 mg/L**	**50 mg/L**	**100 mg/L**	**25 mg/L**	**50 mg/L**	**100 mg/L**	**25 mg/L**	**50 mg/L**	**100 mg/L**
Coefficients of Equation	**Slope**			**$t_{1/2}$**			**Slope**		
	0.0203	0.019	0.021	18.4	31.7	45.2	-0.0598	-0.0688	-0.0244
D_p	8.10^{-9}	$7.5.10^{-9}$	8.610^{-9}	2.10^{-15}	$1.4.10^{-15}$	1.0310^{-15}	$9.4.10^{-15}$	$1.06.10^{-14}$	$3.5.10^{-15}$
Equation	**Eq (17)**			**Eq (18)**			**Eq (19)**		
Coefficients of Equation	**$t_{1/2}$**			**Slope**			**Slope**		
	18.4	31.7	45.2	-0.026	-0.0295	-0.0396	0.136	0.133	0.134
D_f	$9.3.10^{-10}$	$3.5.10^{-10}$	$4.3.10^{-11}$	0.059	0.067	0.091	$3.16.10^{-10}$	$3.06.10^{-10}$	$3.08.10^{-10}$

In a study conducted by Shanthi et al. [28] on the removal of reactive red-4 using activated carbon derived from seed shell waste, it was observed that the D_p values ranging from 10^{-9} to 10^{-10} cm^2/s indicated the influence of pore diffusion in the rate-limiting step. These findings are consistent with the results reported by other researchers [19].

Furthermore, in the present study, the obtained diffusion coefficient values (D_p and D_f) for the six equations are of the same magnitude, except for those obtained using eq. (18).

The film diffusion, as indicated by Boyd's eq. (14) [15], exhibits a similar mathematical form to the pseudo first-order eq. (3), making it difficult to discern which model controls the adsorption process. However, when comparing the obtained D_f values from eq. (13) to the range of 10^{-6} to 10^{-8} cm^2/s, it becomes evident that film diffusion predominates as the rate-determining step in the MR adsorption process, rather than the values obtained for D_f.

The D_f values show an increase from 8.8×10^{-7} to 1.8×10^{-6}, from 1.4×10^{-2} to 4.7×10^{-2}, and from 2.02×10^{-9} to 2.3×10^{-9} as the dye concentration increases from 25 to 100 mg/L for eq. (17), (18), and (19), respectively. Similar effects of dye concentration on D_f values were observed in the adsorption of Congo red dye by soil [19]. These findings emphasize the complex nature of MR dye adsorption on brewery waste, involving both film diffusion and pore diffusion mechanisms in determining the rate of adsorption.

Table 4 presents the results obtained for BY dye sorption when applying eq. (14) to (19). The utilization of eq. (15) and (16) yielded diffusion coefficient values that did not fall within the range associated with a process primarily governed by internal diffusion. However, eq. (10) yielded results indicating that internal diffusion might serve as a limiting step. In terms of the external diffusion coefficient, none of the equations ranging from (17) to (19) produced values that suggested its role as a limiting step.

In order to determine the limiting step in the case of BY, it is necessary to calculate the respective time values for both intra-particle diffusion and film diffusion. By comparing the calculated time ratio to 1, we can identify which step is the controlling factor. If the ratio is less than 1, it indicates that intra-particle diffusion governs the process. Conversely, if the ratio is greater than 1, it suggests that the process is controlled by film diffusion [2].

From Fig. 9, the time of each step was determined. The value of time ratio of external and internal diffusion for different dye concentration is evaluated. The obtained values 0.66 was less than 1, which implies that the intra particle diffusion is the dominant step in the BY dye adsorption process.

Conclusion

This study focuses on the adsorption of MR and BY dyes using brewery waste as a low-cost and effective adsorbent. The pseudo first and second order models, which are commonly used in kinetics analysis, were applied to analyze the adsorption process. The results showed that the pseudo second order model provided the best fit to the experimental data. This model was chosen based on its high determination coefficient value (R^2=0.999) and the close agreement between the experimental adsorption capacity (q_{exp}) and the model-predicted adsorption capacity (q_{est}). Furthermore, the coefficients obtained for the relationship between the intra-particle diffusion coefficient and the initial dye concentration were found to be more

significant compared to the coefficients obtained for the relationship between the external diffusion coefficient and the initial dye concentration. The difference in coefficients was 3.2 for the MR dye and 0.13 for the BY dye, indicating the greater influence of initial dye concentration on intra-particle diffusion in the single diffusion resistance case. By applying various equations to analyze the adsorption mechanism of both MR and BY dyes using brewery waste as an adsorbent, it was found that both modes of diffusion play a role in the rate-limiting step. However, the dominant step for both dyes was determined to be film diffusion. In summary, the results indicate that brewery waste, as a low-cost adsorbent, exhibits a higher affinity for MR dye compared to BY dye.

Acknowledgement

Gratefully acknowledge the team of Analytical Chemistry–Laboratory of Valencia University- for their help in carrying out sample analysis

Conflict of Interest

The authors declare that they have no conflicts of interest.

References

1. T. Maiyalagan and S. Karthikeyan, *Ind. J. Chem. Technol.,* 20 (2013) 7. http://hdl.handle.net/123456789/15857
2. C.R. Girish and V.R. Murty, *Int. J. Chem. Eng.,* 2016 (2016) 1. http://dx.doi.org/10.1155/2016/5809505
3. P.K. Ngoc, T.K. Mac, H.T. Nguyen, D. T. Viet, T.D. Thanh, P.V. Vinh, B.T. Phan, A.T. Duong, R. Das,*J. Sci.: Adv. Mat. Dev.,* 6 (2021) 245. https://doi.org/10.1016/j.jsamd.2021.02.006
4. V. Ka-Man Au, *Front. Chem.,* 8 (2020) 1. https://doi.org/10.3389/fchem.2020.00708
5. A. Abdelfattah, V. K. Yadav, S. K. Pathan, B. Singh, H. Osman, N. Choudhary, K. M. Khedher and A. Basnet, *Adsorpt. Sci. Technol.,* 2023 (2023) 1. https://doi.org/10.1155/2023/1532660
6. R. Wolski, A. Bazan-Wozniak and R. Pietrzak, *Molecules*, 28 (2023) 1. https://doi.org/10.3390/molecules28186712
7. F. Ouazani, H. Benchekor, Y. Chergui, A. Iddou and A. Aziz, *J. Environ. Health Sci. Eng.,* 2020 (2020) 1. https://doi.org/10.1007/s40201-020-00526-4
8. F. Ouazani, A. Iddou and A. Aziz, *Desalin. Water Treat.*, 93 (2017) 1. doi:10.5004/dwt.2017.21413
9. P. K. Malik, *Dyes Pigm.,* 56 (2003) 243. http://dx.doi.org/10.1016/S0143-7208(02)00159-6
10. G. McKay, J. F. Porter and G. R. Prasad, *Water Air Soil Pollut.,* 114 (1999) 423. https://doi.org/10.1023/A:1005197308228
11. B. Stephen Inbraj, N. Sulochana, *Ind. J. Chem. Technol.,* 9 (2002) 201. http://hdl.handle.net/123456789/18884
12. J. A. Abudaia, M.O. Sulyman, K.Y. El-Azaby and S.M. Ben-Ali, *Int. J. Environ. Sci. Develop.,* 4 (2013) 192. doi: 10.7763/IJESD.2013.V4.333
13. R. Chikri, N. Elhadiri, M. Benchanaa and Y. Elmaguana, *J. Chem.,* 2020 (2020) 1. https://doi.org/10.1155/2020/8813420
14. G. Avantaggiato, D. Greco, A. Damascelli, M. Solfrizzo and A. Visconti, *J. Agric. Food Chem.*, 62 (2014) 497. dx.doi.org/10.1021/jf404179h
15. Y.S. Ho, J.C.Y. Ng and G. McKay, *Sep. Purif. Method.*, 29 (2000) 189. https://doi.org/10.1081/SPM-100100009

16. S. Zhang, Z. Li, Y. Yang, W. Jian, D. Ma and F. Jia, *Open Phys.,* 18 (2020) 1201. https://doi.org/10.1515/phys-2020-0215
17. G. Yuan, B. Zhao and K. H. Chu, *Environ. Eng. Res.,* 25 (2020) 645. https://doi.org/10.4491/eer.2019.205
18. M. Mamdouh. Nassar, H. Yehia Magdy, A. Daifullah and H. Kelany, *Adsorp. Sci. Technol.,* 26 (2008) 157. https://doi.org/10.1081/SPM-100100009
19. G. Jordana, D. S. P. Franco, M. S. Netto, Y. L. O. de Salomón, D. G. A. Piccilli, E. L. Foletto and G. L. Dotto, *Environ. Sci. Pollut. Res.,* 28 (2021) 20854. https://doi.org/10.1007/s11356-020-11957-9
20. G. Mckay, M. J. Bino and A. Altememi, *Water Res.,* 20 (1986) 435.
21. A. E. Khan, A. Shahjahan and T. A. Khan, *J. Mol. Liq.,* 249 (2018) 1195. https://doi.org/10.1016/j.molliq.2017.11.125
22. A. Khalfaoui, E. M. Bouchareb, K. Derbal, S. Boukhaloua, B. Chahbouni and R. Bouchareb, *Clean. Chem. Eng.,* 4, (2022) 1. https://doi.org/10.1016/j.clce.2022.100069.
23. V. Srivastava, C. H. Weng, V. K. Singh, and Y. C. Sharma, *J. Chem. Eng. Data,* 56 (2011) 1414. https://doi.org/10.1021/je101152b
24. A. M. Hubbe, S. Azizian and S. Douven, *Bio. Resour.,* 14 (2019) 7582. doi: 10.15376/biores.14.3.7582-7626
25. S. M. El-Geundi, *Adsorp. Sci. Technol.,* 7 (1991) 124. doi:10.1177/026361749000700303
26. H. Arslanoğlu, S. Kaya and F. Tümen, *Particul. Sci. Technol.,* 38 (2019) 1. doi: 10.1080/02726351.2019.1632399
27. W. H. Cheung , Y. S. Szeto, G. McKay, *Biores. Technol.,* 98 (2007) 1. doi: 10.1016/j.biortech.2006.09.045
28. P. Shanthi, G. Tamilarasan, K. Anitha and S. Karthikeyan, *Rasayan J. Chem.,* 7 (2014) 229.
29. C. S. Betianu, P. Cozma, M. Ros and E. D. Comanit, *Processes,* 8 (2020) 1. doi:10.3390/pr8121639